Tautomerism in Cytosine and Uracil: An Experimental and Theoretical Core Level Spectroscopic Study

Vitaliy Feyer,[†] Oksana Plekan,[†,+] Robert Richter,[†] Marcello Coreno,[‡] Gemma Vall-llosera,[§] Kevin C. Prince,*[,†,∥] Alexander B. Trofimov,[⊥,#] Irina L. Zaytseva,[⊥] Tatyana E. Moskovskaya,[⊥] Evgeniy V. Gromov,[⊥,¶] and Jochen Schirmer[¶]

Sincrotrone Trieste, in Area Science Park, I-34012 Basovizza (Trieste), Italy, CNR-IMIP, Montelibretti (Rome), I-00016 Italy, Department of Physics, School of Engineering Science, Royal Institute of Technology, 10691-Stockholm, Sweden, Laboratorio Nazionale TASC, INFM-CNR, 34012 Trieste, Italy, Laboratory of Quantum Chemistry, Irkutsk State University, 664003 Irkutsk, Russia, Favorsky Institute of Chemistry, SB RAS, 664033 Irkutsk, Russia, and Theoretische Chemie, Physikalisch-Chemisches Institut, Universität Heidelberg, Im Neuenheimer Feld 229, D-69120 Heidelberg, Germany

Received: February 03, 2009; Revised Manuscript Received: March 12, 2009

The O, N, and C 1s core level photoemission spectra of the nucleobases cytosine and uracil have been measured in the vapor phase, and the results have been interpreted via theoretical calculations. Our calculations accurately predict the relative binding energies of the core level features observed in the experimental photoemission results and provide a full assignment. In agreement with previous work, a single tautomer of uracil is populated at 405 K, giving rise to relatively simple spectra. At 450 K, three tautomers of cytosine, one of which may consist of two rotamers, are identified, and their populations are determined. This resolves inconsistencies between recent laser studies of this molecule in which the rare imino-oxo tautomer was not observed and older microwave spectra in which it was reported.

I. Introduction

Understanding the structure of the five nucleic acid bases (NABs) of DNA and RNA is fundamental to modeling and predicting their behavior in larger molecules, such as nucleosides, nucleotides, and DNA itself. Much effort has been devoted to the spectroscopy of free NABs, where the fundamental molecular properties can be observed without the effects of solvation. Some of these bases exist as tautomers, and it was recognized very early that tautomerism can lead to mutations. In the gas phase and at temperatures of several hundred Kelvin, a few tautomers of guanine and cytosine are significantly populated, whereas thymine, adenine, and uracil each exist in a single form.[1,2] In the experiments described here, we verify the existence and quantify the populations of the tautomeric forms of free cytosine (see Figure 1a) at a known temperature using core level spectroscopy. Choi and Miller[1] have recently quantified the populations of guanine, but to our knowledge there has not been a corresponding experimental verification of the populations and relative Gibbs free energies of cytosine tautomers. For comparison, we have also measured another pyrimidine base, uracil, where only a single tautomer (see Figure 1b) is populated at the temperature of the experiment.

Some controversy exists about the number of tautomers of cytosine in the gas-phase. Szczesniak et al.[3] carried out matrix isolation studies of cytosine evaporated at 493 K onto substrates at 15 K and found two tautomers identified as amino-oxo and amino-hydroxy, numbers 1 and 2 in Figure 1a. (In the present work, where rotamers 2a and 2b are not distinguished experimentally we label them collectively as tautomer 2.) Szczesniak et al.[3] did not observe the tautomer 3. Brown et al.[4] carried out a microwave study of jet-cooled cytosine using a nozzle temperature of 568 K and found three tautomers, corresponding to 1, 2b, and 3 in Figure 1. They estimated the populations to be in the approximate ratio 1:1:0.25, although the use of jet cooling makes it unclear whether the population is frozen into the equilibrium value for 568 K. Nir et al.[5] used laser ablation/jet cooling and resonant multiphoton ionization to study cytosine and some derivatives and found only the forms 1 and 2. Tomić et al.[6] explained this failure to observe the imino-oxo tautomer

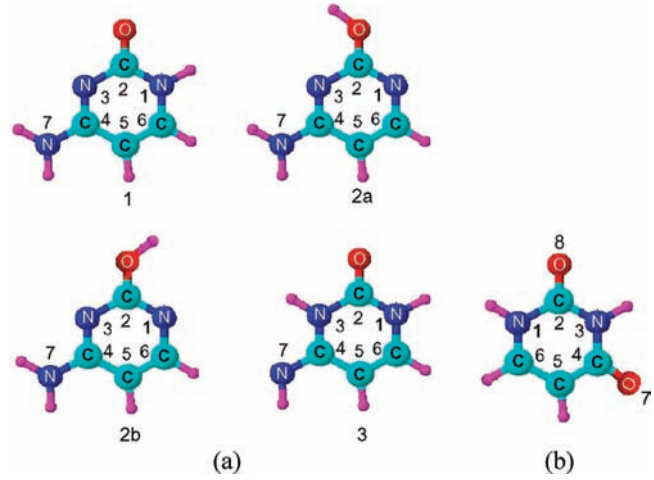

Figure 1. (a) Low-energy tautomers of cytosine and (b) canonical form of uracil.

* Corresponding author. Fax number: +39 040 375 8565. E-mail: Prince@Elettra.Trieste.It.
† Sincrotrone Trieste.
‡ CNR-IMIP.
§ Royal Institute of Technology.
∥ Laboratorio Nazionale TASC.
⊥ Irkutsk State University.
Favorsky Institute of Chemistry.
¶ Universität Heidelberg.
+ Permanent address: Institute of Electron Physics, 88017 Uzhgorod, Ukraine.

10.1021/jp900998a CCC: $40.75
Published on Web 04/21/2009

3 in terms of a low transition moment. It is also possible that in the laser ablation experiment this tautomer is not populated because of the method of sample preparation; in the solid state, cytosine exists as tautomer 1, and laser ablation is a highly nonequilibrium process. Choi et al.[7] observed tautomers 1, 2a, and 2b and obtained preliminary evidence of the imino form 3, but stated that "more convincing evidence" was necessary. However, they calculated that the energy of tautomer 3 was 67 kJ/mol above that of the lowest-energy tautomer, making it unlikely that it would be populated significantly. Choi et al. reanalyzed the microwave data of Brown et al. and found that it was more consistent with the observation of tautomers 1 and 2 than with the original assignment of 1, 2b, and 3. The question of why three tautomers were observed in the very early study of Brown et al. but not in more recent studies is, thus, open, although plausible explanations exist. Evidently there is a need to resolve this question.

There have been many theoretical studies of the ground-state tautomers of cytosine, particularly of their total energy, and the fairly recent ones of Hanus et al.,[8] Trygubenko et al.,[9] and Fogarasi[10] used the second order Møller−Plesset perturbation theory (MP2) and coupled cluster techniques. The first authors used a series of basis sets that made possible extrapolation of the results to the infinite basis set limit. Both Hanus et al. and Trygubenko et al. predicted that the most stable form is tautomer 2b, followed by 2a, 1, and 3 (note that Trygubenko et al. inverted the labeling of the rotamers 2a and 2b with respect to the notation used here and by Fogarasi). Fogarasi carried out less extensive calculations but reported energies calculated at several temperatures.

Laser or microwave spectroscopy studies of laser-ablated and jet-cooled samples have been invaluable in identifying the basic tautomeric structures of NABs, although there is some disagreement on assignments. However, since the intensity of the measured signals is not directly proportional to the tautomer populations, for the determination of the latter, demanding calculations of relative cross sections are needed. The outcome of these calculations may strongly influence the analysis of the experimental results. This is exemplified by the reinterpretation of the guanine spectra of Choi and Miller[1] by Marian[11] and, as mentioned above, the reinterpretation of the cytosine spectra of Nir et al.[5] by Tomić et al.[6] Both laser vaporization and jet cooling of the sample are nonequilibrium processes, so the measured tautomer populations are not necessarily related to equilibrium thermodynamic parameters. In spectroscopic methods using low temperatures, such as matrix isolation and helium droplet studies, the evaporation temperature is known, and it is assumed that the activation barrier between different tautomers is high, so that the populations at the evaporation temperature are frozen into the low-temperature sample. This is probably a good assumption, but it has not been tested for cytosine. As a result of these complications, there is very little data on equilibrium thermodynamic parameters of NABs in the gas phase.

In the following, we apply core level photoemission spectroscopy to study thermally evaporated cytosine and uracil vapors. This method has the advantages that the sample is in thermal equilibrium, the core level photoemission intensity is very nearly directly proportional to the population of the corresponding chemical state, and our calculations provide assignments and can correct for small differences in intensity due to variations in pole strength. Valence level photoemission has been applied to NABs where cross sections are high,[12] and core level spectroscopy has been applied to study tautomers of some volatile smaller molecules,[13,14] but core spectroscopy of NABs is more difficult. They are thermally sensitive, so careful sample preparation is needed. We have recently reported core level spectra and detailed calculations for adenine and thymine,[15] and, in the present work, we extend our studies to cytosine and uracil. Our results for guanine will be reported elsewhere.

II. Experimental and Theoretical Methods

Experimental Section. The experimental methods have been described in detail elsewhere.[15] The samples were obtained from Sigma-Aldrich with a minimum purity of 99% and used without any further purification. They were checked before the experiment using photoionization mass spectroscopy to ensure that there was no evidence of thermal decomposition. The same furnace was used for these checks and for the experiment, and the evaporation temperatures were 450 K for cytosine and 405 K for uracil. The spectra were measured at the gas-phase photoemission beamline, (Elettra, Trieste)[16] using the same apparatus as described previously.[15] To check the quality of the samples during the experiment, valence spectra were taken at 99 eV photon energy. The cytosine spectra were consistent with those of Trofimov et al.,[12] and the peak energies of uracil were consistent with those of Dougherty et al.[17] taken at 21.2 eV. The relative peak intensities were different due to different cross sections at 21.2 and 99 eV. The spectra remained constant over the course of the experiment and did not show evidence of decomposition products, such as water or carbon dioxide, which are easily identified in valence spectra.

The C 1s, N 1s, and O 1s core photoemission spectra were taken at 382, 495, and 628 eV photon energy, respectively, and the binding energy was calibrated to the 1s energies of N_2 and CO_2.[18,19] The spectra were measured with a total resolution (photons + analyzer) of 0.20, 0.32, 0.46, and 0.53 eV at photon energies 99, 382, 495, and 628 eV, respectively.

Theoretical Approach. Essentially the same theoretical approach as in our previous study of thymine and adenine[15] was employed, and we summarize here only the main details. The energies (Ω_t) and the relative intensities (P) of the vertical ionization transitions were computed using the fourth-order algebraic-diagrammatic construction (ADC(4)) approximation scheme for the one-particle Green's function[20−22] adapted for the case of K-shell ionization by means of an additional core−valence separation (CVS) approximation.[23,24] The relative intensities P, also referred to as "pole strengths", represent the result of the Green's function theory applied to molecular electronic structure and do not contain any X-ray photoelectron spectroscopy (XPS)-specific cross-section effects,[20−24] such as the variation of cross section with photon energy. However, the variation of the kinetic energy of the photoelectrons is small in the present spectra, so cross-sectional variations are expected to be negligible. The 6-31G basis sets[25,26] were used in the calculations. The ionization spectra were calculated using the ADC(4)/CVS one-particle Green's function code[27] interfaced to the GAMESS (U.K.)[28] program package.

The ground-state molecular structures of cytosine and uracil were obtained by means of full geometry optimization procedures in which density functional theory (DFT) with the B3LYP potential[29] and 6-311G** basis sets[30] was employed. The calculations were carried out using the Gaussian program.[31]

The theoretical spectra of cytosine were constructed as Boltzmann population ratio (BPR) weighted sums over all tautomers. The BPRs were derived from previous theoretical data[9,10] and extrapolated to the temperature of the experiment. The present theoretical ionization intensities $I_t = P \times$ BPR were

TABLE 1: BPRs of Cytosine Tautomers for $T = 298$ and 450 K and Calculated Relative Free Energy G

	Trygubenko et al.[9]		Fogarasi[10]		G (kJ/mol)[a]
tautomer	298 K	450 K[b]	298 K	450 K[c]	450 K
1	0.21	0.29	0.13	0.21	1.39
2a	0.18	0.19	0.16	0.17	2.97
2b	0.60	0.42	0.57	0.39	0.00
3	0.01	0.10	0.14	0.23	5.38

[a] Relative free energy G at 450 K based on the free energy calculated at 298 K by Trygubenko et al.[9] and the temperature dependence predicted by Fogarasi.[10] [b] Values (obtained and used in this work) calculated as explained in footnote[a] (above). [c] Values interpolated from the data of Fogarasi.[10]

normalized so that the sum of intensity was equal to the number of atoms in the molecule, i.e., 1 for oxygen, 3 for nitrogen, and 4 for carbon. The spectral envelopes were generated by convoluting the discrete transition lines with Lorentzian functions. The values of the Lorentzian widths were selected to best match the experimental intensity, and, in an approximate manner, they account for experimental resolution, unresolved vibrational structure, and natural lifetimes of the respective core-hole states.

Thermochemistry of Cytosine Tautomers. The BPRs derived from the theoretical studies by Trygubenko et al.[9] and Fogarasi[10] are compared in Table 1 for $T = 298$ and 450 K (the temperature used to evaporate the sample). Trygubenko et al. did not calculate entropies but reported the Gibbs free energy at 298 K, so we have extrapolated these energies to the temperature of our experiment using the entropy values of Fogarasi. Both calculations predict tautomer 2b to be the most stable and dominant, whereas the nearly degenerate tautomers 1 and 2a are predicted to be approximately 3−4 times less abundant. Our estimates based on the data of Trygubenko et al. predict a small contribution of tautomer 3 at 450 K (0.10), whereas Fogarasi predicts a larger population (0.23). The BPRs evaluated here were adopted for the subsequent theoretical modeling of the XPS spectra.

III. Results and Discussion

Oxygen 1s Ionization. Figures 2 and 3 show the oxygen 1s photoemission spectra of cytosine and uracil with two peaks and a shoulder in the spectra of cytosine and a single peak in the spectrum of uracil. Cytosine contains only one oxygen atom, so the presence of three features directly indicates the presence of more than one chemical species. Below the measured spectra, the theoretical data are shown as full curves, and the calculations reproduce the experimental XPS energies and intensities very well. The theoretical and experimental spectra were aligned by shifting the former by 1.0 eV to lower energy. The binding energies, relative integral intensities, and assignments are summarized in Tables 2 and 3.

Our results clearly demonstrate that the maximum A and shoulder B of the lowest energy XPS O 1s band of cytosine originate from the ionization of oxo tautomers 1 and 3, respectively. The maximum C at 539.30 eV is assigned to the two closely spaced ionization lines belonging to the hydroxy-type tautomers 2a and 2b. In this pair of rotamers, the electronic structure is only slightly different, and so the ionization energies differ by very little, as expected. The onset of the two-hole, one-particle (2h-1p) satellites in the O 1s spectrum is calculated to occur at about 6 eV higher energy than the main lines, with very low intensity, and, thus, the satellites are not observed in the experimental spectrum. We fitted the experimental spectrum

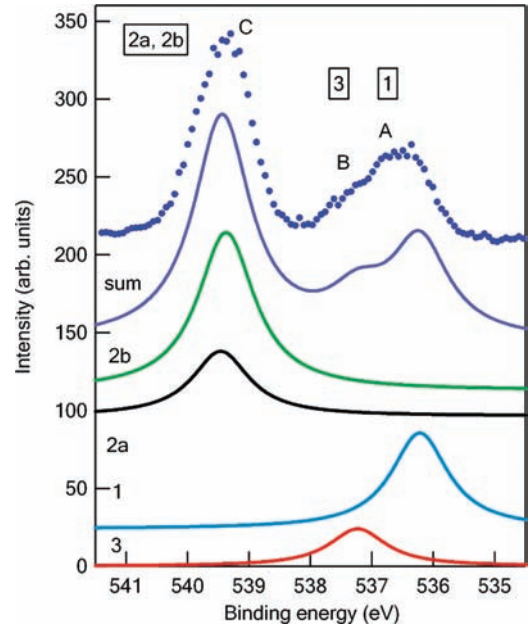

Figure 2. Experimental (points) and theoretical (full curves) O 1s photoionization spectra of cytosine. The theoretical calculations were convoluted with a Lorentzian curve of half-width 0.56 eV and shifted by 1.0 eV to lower binding energy.

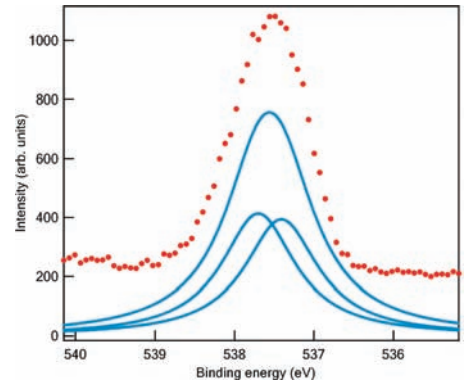

Figure 3. Experimental (points) and theoretical (full curves) O 1s photoionization spectrum of uracil. The theoretical calculations were broadened by a Lorentzian curve of half-width of 0.56 eV and shifted by 0.9 eV to lower binding energy.

TABLE 2: Calculated and Experimental O 1s Ionization Energies and Intensities of Cytosine

	theory				experiment	
tautomer	Ω_t (eV)[a]	P	I_t[b]	feature	Ω_e (eV)	I_e[b]
1	536.22	0.518	0.266	A	536.5	0.26
3	537.23	0.535	0.095	B	537.3	0.11
2b	539.43	0.590	0.440	C	539.4	0.63
2a	539.46	0.589	0.199			

[a] The theoretical ionization energies have been shifted by 1.00 eV to lower binding energy. [b] The sums of intensities have been normalized to 1.

with three Gaussian peaks, with the widths and energies as free parameters, and obtained the experimental intensities I_e shown in Table 2.

For uracil, Figure 3, our calculations predict that the two nonequivalent oxygen core levels give rise to two closely spaced lines only 0.29 eV apart (Table 3), resulting (after convolution) in one broad peak. This is in agreement with the experiment where also only a single maximum at 537.6 eV is observed.

TABLE 3: Calculated and Experimental O, N, and C 1s Ionization Energies and Intensities of Uracil

theory			experiment		
transition	Ω_t (eV)[a]	P	feature	Ω_e (eV)	I_e[b]
$(O_7\ 1s)^{-1}$	537.41	0.508	–	537.6	–
$(O_8\ 1s)^{-1}$	537.70	0.533			–
$(N_3\ 1s)^{-1}$	406.50	0.598	–	406.8	–
$(N_1\ 1s)^{-1}$	406.92	0.588			–
$(C_5\ 1s)^{-1}$	290.86	0.574	A	291.0	0.58
$(C_6\ 1s)^{-1}$	292.78	0.591	B	292.8	0.57
$(C_4\ 1s)^{-1}$	294.41	0.602	C	294.4	0.56
$(C_2\ 1s)^{-1}$	295.54	0.615	D	295.4	0.66

[a] The theoretical O, N, and C 1s ionization energies have been rigidly shifted by 0.90, 1.31, and 1.61 eV, respectively, to lower binding energy. [b] The sum of experimental C 1s intensities has been normalized to the sum of the pole strengths, P.

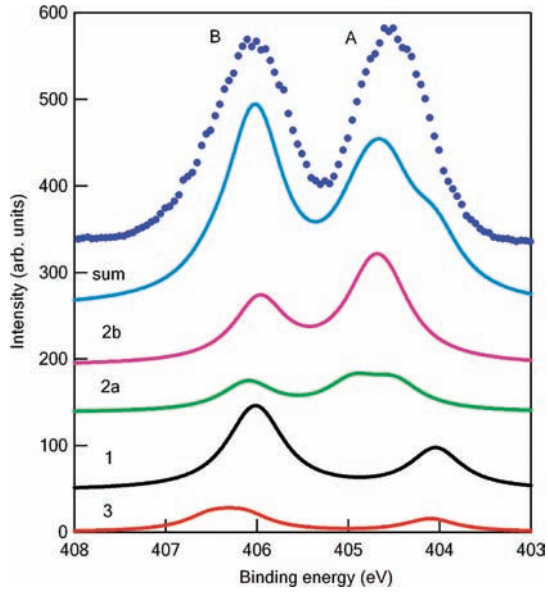

Figure 4. Experimental (points) and theoretical (full curves) N 1s photoionization spectra of cytosine. The theoretical calculations were convoluted with a Lorentzian curve of half-width of 0.35 eV and shifted by 1.31 eV to lower binding energy.

These results confirm the absence of oxo-hydroxy tautomerism at the experimental temperature of 405 K. The data are summarized in Table 3.

Nitrogen 1s Ionization. There are three nitrogen atoms in cytosine, and its N 1s ionization spectrum in Figure 4 consists of two intense maxima A and B centered at 404.5 and 406.1 eV, respectively. The four tautomers of cytosine, each with three nonequivalent nitrogen atoms, can in principle give rise to a total of 12 ionization lines, but these N 1s lines are distributed between just two spectral regions related to ionization of imino- and amino-type nitrogen atoms. The lower energy group of transitions A comprises the signals of the imino-type nitrogen atoms (N_3 in tautomer 1, N_3 and N_1 in 2a and 2b, N_7 in 3), whereas the signals of the amino-type nitrogen atoms (N_1 and N_7 in tautomer 1, N_7 in 2a and 2b, N_3 and N_1 in tautomer 3) are found in the higher energy part of the spectrum. The individual contributions are indicated in Figure 4 as curves for each tautomer, and the data are summarized in Table 4. For tautomer 2a, all three core levels can be discerned in the theoretical curve, whereas for 1 and 3 the two amino nitrogen core levels are unresolved and give rise to a peak roughly twice as intense as the imino contribution. For tautomer 2b, this trend is reversed and the imino peak is about twice as intense as the amino peak.

The present theoretical spectrum qualitatively reproduces the experimental spectral profile, and the most obvious difference between theory and experiment is the difference in peak height. However, the ratios of the integral intensities of the bands in the theoretical and experimental spectra are consistent and equal to 1.55:1.45 and 1.47:1.53, respectively, representing a discrepancy of only 5%. The difference in peak height occurs because the calculation slightly overestimates the differences in energy of the components of peak A, causing it to broaden. In addition, we have not modeled the vibrational envelope, which may vary between different core levels.

The N 1s ionization spectrum of uracil, Figure 5, consists of a single peak, and our theoretical calculations reproduce this feature observed at 406.8 eV in the experiment. The calculations show a small difference, 0.42 eV, between the binding energies of the N_3 and N_1 atoms, which are both secondary amino nitrogen atoms. The small shift is the result of a number of initial-state chemical and final-state screening effects. From cytosine, we know that amino-imino tautomerism causes a substantial core level shift, so the absence of intensity at 404−405 eV confirms the absence of this form of tautomerism, as expected. The results are summarized in Table 3.

Carbon 1s Ionization. The ionization of the four carbon atoms in each of the four tautomers of cytosine can, in principle, give rise to 16 main lines in the C 1s spectrum of cytosine. In practice, the spectrum exhibits six distinct maxima (A−F), which can only be assigned with information from calculations, Figure 6. The calculated spectrum is in very good qualitative agreement with the experimental results. The observed differences are more quantitative than qualitative and include an overall shift of the theoretical spectrum by 1.55 eV and an apparent high-energy shoulder of band E. This appears to be due to an overestimate of the difference in energy between C_2 in tautomer 1 and C_2 in 2a and 2b (Table 5).

The lowest band A at 290.58 eV contains signals from the C_5 atoms of all four tautomers. This atom is situated in the middle of the aromatic $C_4-C_5-C_6$ fragment, which is common to all tautomers, and has the lowest binding energy of any C atom. Ionization of C_6 atoms does not give rise to a single peak, but rather two peaks B (from tautomers 2a + 2b) and C (from tautomers 1 + 3) at 291.71 and 292.40 eV, respectively. The lower binding energy (relative to the other tautomers) of C_6 in tautomers 2a and 2b is related to the fact that the C_6 atom is adjacent to the imino-type nitrogen N_1, which in tautomers 1 and 3 becomes an amino-type N atom with a lower degree of aromaticity.

Peak D at 293.21 eV includes signals from the C_4 atoms. These atoms have a similar environment in all four tautomers and thus form a single compact group of lines.

In tautomer 3, the C_2 atom is between the two amino-type nitrogen atoms and, thus, appears to be completely isolated from the aromatic system. Moreover, the electronic density at C_2 is depleted by charge transfer to oxygen and, to a lesser extent, nitrogen. The C_2 core level, therefore, has a large chemical shift and appears as the peak F at 295.30 eV, which is separated from the other C_2 transitions by an energy of over 1 eV. The calculations seem to slightly overestimate this shift.

For the integral intensities of the individual peaks, the agreement of peaks A and F with theory is striking and confirms the accuracy of the thermodynamic calculations. Peaks B−E deviate by about 15% from the predicted values. This is probably due to the crudeness of the fit for estimating the integral

TABLE 4: Calculated and Experimental N 1s Ionization Energies and Intensities of Cytosine

theory						experiment		
tautomer	transition	Ω_t (eV)[a]	P	I_t[b]	sum I_t	feature	I_e	Ω_e (eV)
1	$(N_3\ 1s)^{-1}$	404.04	0.550	0.283				
3	$(N_7\ 1s)^{-1}$	404.10	0.507	0.090				
2a	$(N_1\ 1s)^{-1}$	404.49	0.532	0.179	1.55	A	1.47	404.5
2b	$(N_1\ 1s)^{-1}$	404.58	0.534	0.397				
2b	$(N_3\ 1s)^{-1}$	404.77	0.557	0.415				
2a	$(N_3\ 1s)^{-1}$	404.95	0.559	0.188				
1	$(N_7\ 1s)^{-1}$	405.95	0.590	0.305				
2b	$(N_7\ 1s)^{-1}$	405.97	0.594	0.442				
1	$(N_1\ 1s)^{-1}$	406.09	0.567	0.291	1.45	B	1.53	406.1
2a	$(N_7\ 1s)^{-1}$	406.10	0.595	0.200				
3	$(N_3\ 1s)^{-1}$	406.14	0.599	0.106				
3	$(N_1\ 1s)^{-1}$	406.49	0.586	0.104				

[a] Theoretical ionization energies have been shifted by 1.31 eV to lower binding energy. [b] Sums of intensities have been normalized to 3.

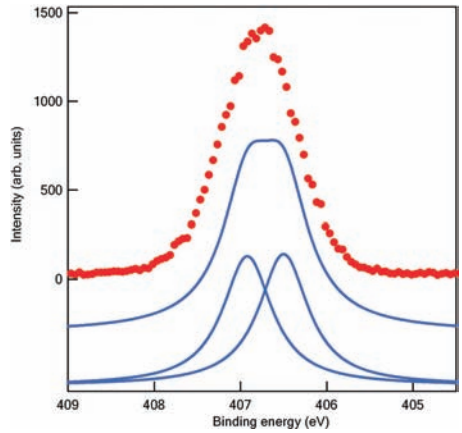

Figure 5. Experimental (points) and theoretical (full curves) N 1s photoionization spectra of uracil. The theoretical calculations were convoluted with a Lorentzian curve of half-width of 0.35 eV and shifted by 1.2 eV to lower binding energy.

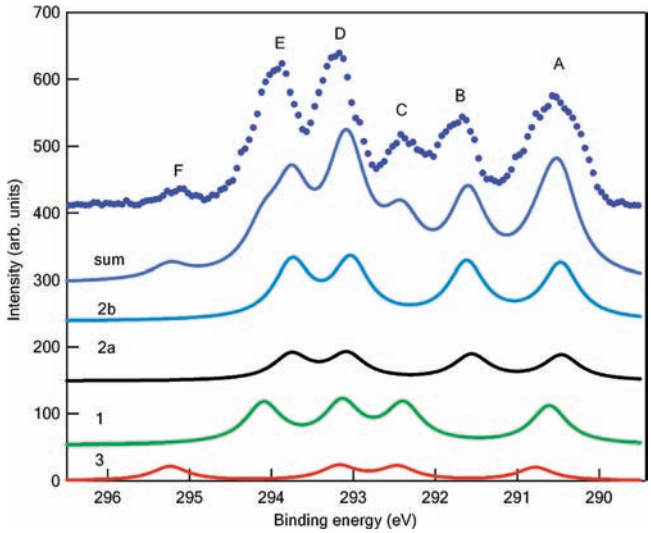

Figure 6. Experimental (points) and theoretical (full curves) C 1s photoionization spectra of cytosine. The theoretical calculations were convoluted with a Lorentzian curve of half-width 0.26 eV and shifted by 1.55 eV to lower binding energy.

intensities, namely a fit with a symmetric Gaussian whereas vibrational envelopes are often asymmetric. If peaks B and C are summed to give the contribution of C_6 atoms in all four tautomers, then the agreement with experiment is very good.

The C 1s spectrum of uracil (Figure 7) consists of four maxima A−D at 290.96, 292.83, 294.44, and 295.40 eV, respectively, which are related to ionization of the four carbon atoms in the molecule. Our calculations are in very good agreement with the experimental data, and the peaks A−D are assigned to the C_5, C_6, C_4, and C_2 atoms, respectively, Table 3. The widths have been set equal in the simulation, but they vary by about ±10% experimentally, reflecting different Franck−Condon factors for each core level. The C 1s chemical shifts here are quite similar to those observed in cytosine, and their interpretation is closely analogous.

It is worth noting the similar environment of C_2 in uracil and tautomer 3 of cytosine, which should result in similar chemical shifts for this atom in these species. Indeed, this is seen to be the case by comparing the energy of peaks F in Figure 6 and D in Figure 7. This confirms the assignment of peak F in the spectrum of cytosine and resolves the issue of the presence of tautomer 3 mentioned in the Introduction.

An interesting finding is the monotonic increase in intensity of the four C 1s ionization peaks as a function of binding energy, predicted by theory and tested in the experimental spectrum. The calculated pole strengths for the main C 1s transitions grow from 0.57 to 0.62 indicating stronger many-body (electron correlation) effects for transitions with lower energies. However, this is only partly reflected in the experimental data, Table 5, with peak D being the most intense and the other peaks being about equal.

In the above discussion, we have shown that there is very good agreement between theory and experiment with respect to the intensity of the peaks in the O1s, N1s, and C1s spectra. This suggests that the populations calculated at 450 K (Table 1, Trygubenko et al.) are correct to within about 10% of the value of each population. For all core levels, the energy differences between tautomers 2a and 2b cannot be experimentally resolved, so we cannot determine the relative populations of these rotamers, but the measurement of the ratio 1:(2a+2b):3 is still a stringent test of theory. On comparison with the theoretical free energy calculations by Fogarasi,[10] we find reasonable agreement with his calculations of the relative energies (and, therefore, populations) of tautomers 1 and 2, but the population of tautomer 3 is considerably overestimated. The data are consistent with the electronic energy calculated by Trygubenko et al. and the entropy calculated by Fogarasi, which give a Gibbs free energy of 5.4 kJ/mol at 450 K relative to tautomer 2b.

The data show that the explanation of Tomić et al.[6] for the absence of the imino tautomer in the spectra of Nir et al.[5] is plausible, as at least, under the present thermal equilibrium conditions, the tautomer is populated. The original microwave

TABLE 5: Calculated and Experimental C 1s Ionization Energies and Intensities of Cytosine

theory						experiment		
tautomer	transition	Ω_t (eV)[a]	P	I_t	sum I_t[b]	feature	I_e	Ω_e (eV)
2a	$(C_5\ 1s)^{-1}$	290.46	0.572	0.187				
2b	$(C_5\ 1s)^{-1}$	290.47	0.573	0.413	0.985	A	0.98	290.6
1	$(C_5\ 1s)^{-1}$	290.61	0.576	0.287				
3	$(C_5\ 1s)^{-1}$	290.78	0.572	0.098				
2a	$(C_6\ 1s)^{-1}$	291.56	0.575	0.188	0.603	B	0.52	291.7
2b	$(C_6\ 1s)^{-1}$	291.62	0.575	0.415				
1	$(C_6\ 1s)^{-1}$	292.39	0.574	0.286	0.386	C	0.47	292.4
3	$(C_6\ 1s)^{-1}$	292.46	0.580	0.100				
2b	$(C_4\ 1s)^{-1}$	293.03	0.588	0.424				
2a	$(C_4\ 1s)^{-1}$	293.08	0.584	0.190	1.02	D	0.89	293.2
1	$(C_4\ 1s)^{-1}$	293.14	0.595	0.296				
3	$(C_4\ 1s)^{-1}$	293.18	0.611	0.105				
2b	$(C_2\ 1s)^{-1}$	293.75	0.581	0.419				
2a	$(C_2\ 1s)^{-1}$	293.76	0.578	0.189	0.907	E	1.05	293.9
1	$(C_2\ 1s)^{-1}$	294.10	0.601	0.299				
3	$(C_2\ 1s)^{-1}$	295.24	0.618	0.106	0.106	F	0.10	295.1

[a] Theoretical ionization energies have been shifted by 1.55 eV to lower binding energy. [b] Theoretical Boltzmann-weighted photoelectron intensities. The sum has been normalized to 4.

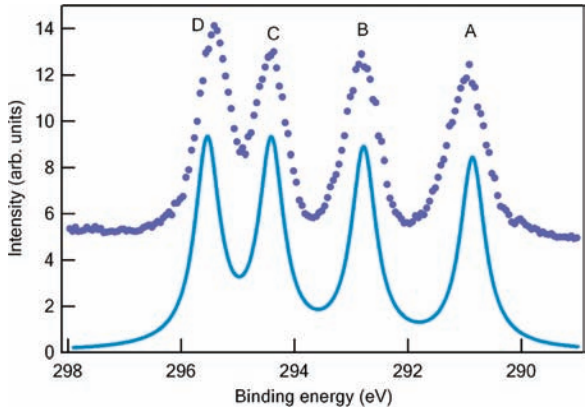

Figure 7. Experimental (points) and theoretical (full curve) C 1s photoionization spectra of uracil. The theoretical calculations were convoluted with a Lorentzian curve of half-width 0.26 eV and shifted by 1.6 eV to lower binding energy.

work of Brown et al.[4] correctly identified this tautomer and its population, but estimated only approximately the ratio of tautomers. Even at the higher temperature of that study, the BPR is not equal to their estimated value of 1:1:0.25. This suggests the previous data, in particular the calculated energy for tautomer 3 (67 kJ/mol),[7] need to be revised. Clearly, we have provided the "convincing evidence" that they mentioned for the existence of this tautomer.

IV. Conclusions

We have measured the core photoemission spectra of cytosine and uracil tautomers at temperatures of 450 and 405 K, respectively. Uracil exists as a single tautomer, and the spectra are well reproduced by our calculations. The tautomers of cytosine can be identified in both the O and C 1s spectra, and the equilibrium population was estimated, while N 1s spectra provided an additional check of the correctness of the population estimate. The failure to observe the imino tautomer 3 in recent laser studies is probably due to low transition moments. The calculated electronic energies of Trygubenko et al.[9] combined with the calculated entropy of Fogarasi yield accurate values of the Gibbs free energies at 450 K.

Acknowledgment. The theoretical part of this study was supported by grants of the Russian Foundation for Basic Research (RFBR) and the Deutsche Forschungsgemeinschaft (DFG). We thank our colleagues at Elettra for providing good quality synchrotron light. O. Plekan acknowledges financial support from the Area di Ricerca di Trieste under the Incoming Mobility scheme. V. Feyer acknowledges financial support from the Abdus Salaam International Center for Theoretical Physics for a TRIL (Training and Research in Italian Laboratories) fellowship. A.B. Trofimov acknowledges support from the Alexander von Humboldt Foundation. The authors are indebted to Profs. L. S. Cederbaum, V. B. Kobychev, and N. M. Vitkovskaya for interest in this work and valuable discussions.

References and Notes

(1) Choi, M. Y.; Miller, R. E. *J. Am. Chem. Soc.* **2006**, *128*, 7320–7328.
(2) Choi, M. Y.; Miller, R. E. *J. Phys. Chem. A* **2007**, *111*, 2475–2479.
(3) Szczesniak, M.; Szczesniak, K.; Kwiatowski, J. S.; KuBulat, K.; Person, W. B. *J. Am. Chem. Soc.* **1988**, *110*, 8319–8330.
(4) Brown, R. D.; Godfrey, P. D.; McNaughton, D.; Pierlot, A. P. *J. Am. Chem. Soc.* **1989**, *111*, 2308–2310.
(5) Nir, E.; Müller, M.; Grace, L. I.; de Vries, M. S. *Chem. Phys. Lett.* **2002**, *355*, 59–64.
(6) Tomić, K.; Tatchen, J.; Marian, C. M. *J. Phys. Chem. A* **2005**, *109*, 8410–8418.
(7) Choi, M. Y.; Dong, F.; Miller, R. E. *Philos. Trans. R. Soc. London, Ser. A* **2005**, *363*, 393–413.
(8) Hanus, M.; Ryjáček, F.; Kabeláč, M.; Kubar, T.; Bogdan, T. V.; Trygubenko, S. A.; Hobza, P. *J. Am. Chem. Soc.* **2003**, *125*, 7678–7688.
(9) Trygubenko, S. A.; Bogdan, T. V.; Rueda, M.; Orozco, M.; Luque, F. J.; Sponer, J.; Slaviček, P.; Hobza, P. *Phys. Chem. Chem. Phys.* **2002**, *4*, 4192–4203.
(10) Fogarasi, G. *J. Phys. Chem. A* **2002**, *106*, 1381–1390.
(11) Marian, C. M. *J. Phys. Chem. A* **2007**, *111*, 1545–1553.
(12) Trofimov, A. B.; Schirmer, J.; Kobychev, V. B.; Potts, A. W.; Holland, D. M. P.; Karlsson, L. *J. Phys. B: At., Mol. Opt. Phys.* **2006**, *39*, 305–329.
(13) Brown, R. S.; Tse, A.; Vederas, J. C. *J. Am. Chem. Soc.* **1980**, *102*, 1174–1176.

(14) Francis, J. T.; Hitchcock, A. P. *J. Phys. Chem.* **1994**, *98*, 3650–3657.

(15) Plekan, O.; Feyer, V.; Richter, R.; Coreno, M.; de Simone, M.; Prince, K. C.; Trofimov, A. B.; Gromov, E. V.; Zaytseva, I. L.; Schirmer, *J. Chem. Phys.* **2008**, *347*, 360–375.

(16) Prince, K. C.; Blyth, R. R.; Delaunay, R.; Zitnik, M.; Krempasky, J.; Slezak, J.; Camilloni, R.; Avaldi, L.; Coreno, M.; Stefani, G.; Furlani, C.; de Simone, M.; Stranges, S. *J. Synchrotron Radiat.* **1998**, *5*, 565–568.

(17) Dougherty, D.; Younathan, E. S.; Voll, R.; Abdulnur, S.; McGlynn, S. P. *J. Electron Spectrosc. Relat. Phenom.* **1978**, *13*, 379.

(18) Thomas, T. D.; Shaw, R. W., Jr. *J. Electron Spectrosc. Relat. Phenom.* **1974**, *5*, 1081.

(19) Myrseth, V.; Bozek, J. D.; Kukk, E.; Sæthre, L. J.; Thomas, T. D. *J. Electron Spectrosc. Relat. Phenom.* **2002**, *122*, 57–63.

(20) Schirmer, J.; Cederbaum, L. S.; Walter, O. *Phys. Rev. A: At., Mol. Opt. Phys.* **1983**, *28*, 1237–1259.

(21) von Niessen, W.; Schirmer, J.; Cederbaum, L. S. *Comput. Phys. Rep.* **1984**, *1*, 57.

(22) Schirmer, J.; Angonoa, G. *J. Chem. Phys.* **1989**, *91*, 1754–1761.

(23) Cederbaum, L. S.; Domcke, W.; Schirmer, J. *Phys. Rev. A: At., Mol. Opt. Phys.* **1980**, *22*, 206–222.

(24) Angonoa, G.; Walter, O.; Schirmer, J. *J. Chem. Phys.* **1987**, *87*, 6789–6801.

(25) Hehre, W. J.; Ditchfield, R.; Pople, J. A. *J. Chem. Phys.* **1972**, *56*, 2257–2261.

(26) Clark, T.; Chandrasekhar, J.; Spitznagel, G. W.; Schleyer, P. v. R. *J. Comput. Chem.* **1983**, *4*, 294–301.

(27) One-particle Green's function ADC(4)/CVS code written by G. Angonoa, O. Walter, and J. Schirmer; direct treatment of the first-order matrix elements and diagonalization due to F. Tarantelli. The constant diagram code written by G. Angonoa, O. Walter, and J. Schirmer; further developed by M. K. Scheller and A. B. Trofimov.

(28) Program written by M. F. Guest, J. H. van Lenthe, J. Kendrick, K. Schoffel, and P. Sherwood with contributions from R. D. Amos, R. J. Buenker, M. Dupuis, N. C. Handy, I. H. Hiller, P. J. Knowles, V. Bonacic-Koutecky, W. von Niessen, R. J. Harrison, A. P. Rendell, V. R. Saunders, and A. J. Stone. The package is derived from the original GAMESS code due to M. Dupuis, D. Spangler, and J. Wendoloski. *GAMESS*; NRCC Software Catalog, Lawrence Berkeley Lab, California University, Berkeley; Program No. QG01, Vol. 1, 1980.

(29) (a) Becke, A. D. *J. Chem. Phys.* **1993**, *98*, 5648–5562. (b) Lee, C.; Yang, W.; Parr, R. G. *Phys. Rev. B* **1988**, *37*, 785–789.

(30) Krishnan, R.; Binkley, J. S.; Seeger, R.; Pople, J. A. *J. Chem. Phys.* **1980**, *72*, 650.

(31) Frisch, M. J.; Trucks, G. W.; Schlegel, H. B.; Scuseria, G. E.; Robb, M. A.; Cheeseman, J. R.; Zakrzewski, V. G.; Montgomery,, J. A., Jr.; Stratmann, R. E.; Burant, J. C.; Dapprich, S.; Millam, J. M.; Daniels, A. D.; Kudin, K. N.; Strain, M. C.; Farkas, O.; Tomasi, J.; Barone, V.; Cossi, M.; Cammi, R.; Mennucci, B.; Pomelli, C.; Adamo, C.; Clifford, S.; Ochterski, J.; Petersson, G. A.; Ayala, P. Y.; Cui, Q.; Morokuma, K.; Malick, D. K.; Rabuck, A. D.; Raghavachari, K.; Foresman, J. B.; Cioslowski, J.; Ortiz, J. V.; Baboul, A. G.; Stefanov, B. B.; Liu, G.; Liashenko, A.; Piskorz, P.; Komaromi, I.; Gomperts, R.; Martin, R. L.; Fox, D. J.; Keith, T.; Al-Laham, M. A.; Peng, C. Y.; Nanayakkara, A.; Gonzalez, C.; Challacombe, M.; Gill, P. M. W.; Johnson, B.; Chen, W.; Wong, M. W.; Andres, J. L.; Gonzalez, C.; Head-Gordon, M.; Replogle, E. S.; Pople, J. A. *Gaussian 98, Revision A.7*; Gaussian, Inc.: Pittsburgh, PA, 1998.

JP900998A